RANS K-ω SIMULATION OF 2D TURBULENT NATURAL CONVECTION IN AN ENCLOSURE WITH HEATING SOURCES

MEHDI AHMADI, SEYED ALI AGHA MIRJALILY* AND SEYED AMIR ABBAS OLOOMI

Department of Mechanical Engineering, Yazd Branch, Islamic Azad University, Yazd, Iran.

**Corresponding author: Saa_mirjalily@iauyazd.ac.ir*

(Received: 13th Dec 2018; Accepted: 24th Feb 2019; Published on-line: 1st June 2019)

https://doi.org/10.31436/iiumej.v20i1.1040

ABSTRACT: This study is conducted to investigate turbulent natural convection flow in an enclosure with thermal sources using the low-Reynolds number (LRN) *k-ω* model. This enclosure has a cold source with temperature T_c and a hot source with temperature T_h as thermal sources, other walls of the enclosure are adiabatic. The aim of this study is to predict the effect of change in Rayleigh number, repositioning of cold and hot sources, and thermal sources aspect ratio on the flow field, temperature, and rate of heat transfer. To achieve this aim, the equations of continuity, momentum, energy, turbulent kinetic energy, and kinetic energy dissipation are employed in the case of 2D turbulence with constant thermo-physical properties except the density in the buoyancy term (Boussinesq approximation). To numerically solve these equations, the finite volume method and SIMPLE algorithm are used. According to the modeling results, the most optimal temperature distribution in the enclosure is seen when the hot source is below the cold source. With decreasing distance between hot and cold sources, heat transfer rate increases. The maximal heat transfer rate is derived via study of the heating sources aspect ratio. In constant positions of cold and hot sources on a wall, the heat transfer rate increases with increasing Rayleigh number ($Ra=10^9$-10^{11}).

ABSTAK: Kajian ini dijalankan bagi mengkaji perubahan semula jadi aliran perolakan dalam tempat tertutup dengan sumber haba menggunakan model *k-ω* nombor Reynolds-rendah (LRN). Bekas tertutup ini mempunyai dua sumber haba iaitu sumber sejuk dengan suhu T_c dan sumber panas dengan suhu T_h, manakala dinding lain bekas ini adalah adiabatik. Tujuan kajian ini adalah bagi mengesan perubahan nombor Rayleigh, mengubah sumber sejuk dan panas dan nisbah sumber haba kepada kawasan aliran, suhu dan halaju perubahan haba. Bagi mencapai tujuan tersebut, persamaan sambungan, momentum, tenaga, tenaga kinetik perolakan, dan pengurangan tenaga kinetik telah dilaksanakan dalam kes perolakan 2D dengan sifat fizikal-haba berterusan (malar) kecuali isipadu terma keapungan (anggaran Boussinesq). Bagi menyelesaikan persamaan ini secara berangka, kaedah isipadu terhad dan algorithma MUDAH telah digunakan. Berdasarkan keputusan model, suhu distribusi optimal dalam bekas tertutup dilihat apabila sumber panas adalah kurang daripada sumber sejuk. Dengan pengurangan jarak antara sumber panas dan sejuk, kadar pertukaran haba meningkat. Kadar pertukaran haba maksima telah diperoleh melalui kajian nisbah aspek sumber pemanasan. Kadar pertukaran haba bertambah dengan bertambahnya nombor Rayleigh ($Ra=10^9$-10^{11}), pada posisi tetap sumber sejuk dan panas pada dinding bekas.

KEYWORDS: *heat transfer; turbulent natural convection; k-ω model; enclosure*

1. INTRODUCTION

Many numerical and experimental studies have been conducted on natural convection flows. In the last two decades, many studies have sought to achieve quantitative data on the processes of flow convective heat transfer and its association with many applications inside enclosures [1-2]. The most important and most frequently investigated section of these convections is a rectangular enclosure filled with dry air and two vertical walls at two different temperatures [3-6]. In a rectangular enclosure with height *H*, heat is naturally transferred from the hot wall to the cold wall through the formation of a vortex with slow movement. The movement of the vortex is considered the engine of heat transfer from hot source to cold source. Flow intensity is expressed by Rayleigh number, $Ra=g\beta\Delta TH^3/\alpha\upsilon$, where, H is the enclosure height, β is coefficient of thermal expansion, ΔT is temperature difference between vertical walls, and α and υ are thermal and molecular diffusivities of fluid.

Depending on the Rayleigh number, the flow can be classified as turbulent or laminar [7-9]. A Rayleigh number of less than 10^8 represents laminar flow, and the transient of laminar flow to turbulent occurs at $Ra=10^8$-10^{10}[10].

Natural convection in enclosure was first experimented by Elder [11] and then Giel and Schmidt [12]. In these experiments, water was used instead of air. Cheesewright [13] studied the mean velocity, center temperature, and turbulent variations in natural convection flow in an air-contained enclosure with temperature difference between the walls. He used a standard K-ε model with wall functions to simulate turbulent convection flow in an enclosure with a radiator. In addition, he used the wall functions to calculate K-ε but did not use them to measure velocity and temperature. The selected model made a good prediction of the average flow, which was consistent with previous studies but was weak for modeling turbulence; the Rayleigh number of the enclosure was constant in his study and was considered $3*10^{10}$ with length to height ratio of the enclosure of 1:5. Dafa Alla and Bets [6] studied natural convection flow in a high enclosure with length/height ratio of 1:14 and the Rayleigh number $8.3*10^5$. In this experiment, a laser velocity meter was used to measure velocity and velocity variations and thermocouple to measure temperature and temperature variations. Olsen et al [14] conducted a study on natural convection flow in an air-conditioning enclosure with a small model and Rayleigh number of 10^{10}. The length/height ratio of the enclosure was approximately 1:3. They illustrated the measured flow and temperature in the center and boundary layer. Unlike previous studies, two lateral lobes were seen in these experiments, this study was a rare study on an enclosure with virtually real dimensions.

Chen [15] used different Reynolds models of stress (RMS) to calculate the natural, forced, and mixed convection flows in the enclosure. Modeling results demonstrated that the efficiency of different RMS approaches to simulate convection flow in the enclosure were equal and consistent with the mean flow derived in experimental calculations, but turbulence values were not predicted appropriately. Ince and Launder [16] studied natural convection flow in a square enclosure with hot right surface and cold left surface and upper and lower adiabatic surfaces. They managed to develop a model to resolve turbulent flow with Rayleigh numbers ranging from 10^6 to 10^{10}. Hanjealic and Vasc [17] used three-equation K-ε-ɵ and four-equation V_1-ε-ɵ-εɵ and low Reynolds number (LRN) to calculate turbulent convection flow in different empty and partitioned enclosures. The Rayleigh number in their studies varied between 10^{10} and 10^{12}, which is compatible with Rayleigh numbers in real indoors. Mean temperature and velocity derived for these models have displayed relatively acceptable consistency with experimental values. Sigey et al. [18]

used Launder and Sharma K-ε model with the wall functions and considered the Rayleigh number of the enclosure 10^{11} in their experiments. Their model was found to optimally predict the flow inside the enclosure; and the values of velocity and temperature derived for all regions of the enclosure were highly consistent with the experimental values. Ji [19] discussed the modelling of natural convection in air cavities using four turbulence models. Regarding the cited studies, we set the aims of the present study. The results of resolving this question can be used in induced buoyancy flows, heat transfer of free convection, and designing and assessing different technical and engineering uses especially designing the systems of central heating and air conditioning. Following the studies of these researchers, in the present paper we investigate turbulent natural convection flow in an enclosure with thermal sources using the low-Reynolds number (LRN) *k-ω* model. The aim of this study is to predict the effect of change in Rayleigh number, repositioning of cold and hot sources and thermal sources aspect ratio on the flow field, temperature, and rate of heat transfer that have been seen less in previous studies. The geometry of this paper is an enclosure that has a cold source with temperature T_c and a hot source with temperature T_h as thermal sources that are placed on the left wall of enclosure, the other walls are adiabatic. Subsequently, to achieve the desired results, the Rayleigh number varies between 10^9-10^{11}.

2. MODEL AND SIMULATION

2.1 Mathematical Model

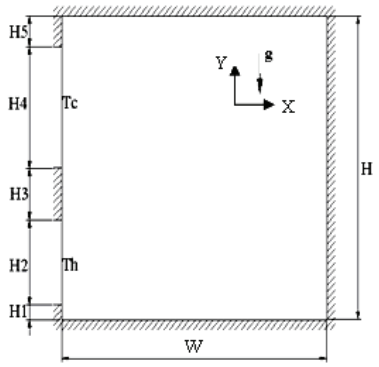

Fig. 1: The geometry of problem.

In the present study, natural convection flow is studied in a 2D enclosure seen in Fig. 1. The temperatures of the cold and hot sources are T_c and T_h, respectively, and other parts are assumed insulated. The aim of this study is to predict the effect of change in Rayleigh number, repositioning of cold and hot sources, and heating sources aspect ratio on the basic parameters of flow and temperature. Therefore, first, the flow field and fluid temperature in the enclosure are determined using a numerical solution, and then the Nusselt number, mean velocity, and temperature are calculated in different sections of the enclosure. To achieve this purpose, turbulent flow in the 2D enclosure is examined. The numerical solution of the question is conducted using a SIMPLE algorithm and the computer program is written using FORTRAN language. Henkes et al. [20] studied the concepts of the critical Rayleigh number of enclosures' layers using natural convection flow. The critical Rayleigh number was derived around 10^{11} for upper Reynolds models and approximately 10^9 for lower ones. If the Rayleigh number is less than 10^8, the flow is laminar, if the Rayleigh number is bigger than 10^{10}, the flow is turbulent, and if the Rayleigh number is 10^8-10^{10}, the flow is transient [8, 21]. Therefore, the Rayleigh number in the question of interest is 10^9-10^{11} and therefore convection flow in the enclosure is

transient. Given the operating conditions of the enclosure, the indoor flow can be laminar or turbulent. This study investigates turbulent flow.

2.1.1 The Equations of Natural Convection Flow in the Enclosure

Turbulent flow field in an enclosure is derived by continuity, momentum, and energy equations. To include buoyancy effects, a Boussinesq approximation was used. Air density, except for buoyancy sentence, is constant and is calculated according to the gases law, and its effects were included in the momentum equation. The enclosure's air was assumed to be incompressible and newtonian (Pr=0.71), and dynamic viscosity was calculated through the Sutherland formula. The equations governing continuity, momentum and energy can be expressed as follows [22]:

$$\frac{\partial}{\partial X_j}(\rho U_j) = 0 \tag{1}$$

$$\frac{\partial(\rho U_i U_j)}{\partial X_j} = -\frac{\partial P}{\partial X_j} + \frac{\partial}{\partial X_j}(\mu \frac{\partial U_i}{\partial X_j} - \rho\overline{u_i u_j}) + \rho g_i \beta(T_{ref} - \mathrm{T}) \tag{2}$$

$$\frac{\partial(\rho C_p U_j T)}{\partial X_j} = \frac{\partial}{\partial X_j}(k \frac{\partial T}{\partial X_j} - \rho\overline{t u_i}) \tag{3}$$

Where U, P, and T represent velocity, pressure, and mean time temperature, respectively. In addition, there are number of high-ranking statements as $\rho\overline{u_i u_j}$, $\rho\overline{u_i t}$ in Reynolds averaging equations, namely, Reynolds stress and turbulent heat transfer, respectively. We conducted turbulent modeling to use the equations of appropriate transfer in order to model these statements.

2.1.2 Two-Equation Model k-ω

There are different turbulence models to solve turbulent flow equations. Here, a standard two-equation model *k-ω* was used in this study. In this model, in addition to a turbulence kinetic energy equation k, an additional differential model solves for energy dissipation.

Wilcox [23] extended low Reynolds model *k-ω* to simulate a transient area as illustrated below. To describe the field and determine turbulence rate in a steady flow, the equations of kinetic energy and those of energy dissipation are generally as follows according to the above formulated hypotheses:

$$\frac{\partial(\rho u_j k)}{\partial X_j} = P_k - \prod_k + \frac{\partial}{\partial X_j}\left[(\mu + \frac{\mu_t}{\sigma_k})\frac{\partial K}{\partial X_j}\right] + S_k \tag{4}$$

$$\frac{\partial(\rho u_j \omega)}{\partial X_j} = P_\omega - \prod_\omega + \frac{\partial}{\partial X_j}\left[(\mu + \frac{\mu_t}{\sigma_\omega})\frac{\partial K}{\partial X_j}\right] + S_\omega \tag{5}$$

$$\mu_t = C_\mu f_\mu \frac{\rho K}{\omega} \tag{6}$$

$$P_k = 2\mu_t S_{ij} \frac{\partial \mathrm{u_i}}{\partial \mathrm{x_j}} \tag{7}$$

$$G_k = -g\beta \frac{\mu_t}{\sigma_t} \frac{\partial T}{\partial \mathrm{x_j}} S_{2j} \qquad S_{ij} = \frac{1}{2}\left(\frac{\partial u_i}{\partial u_j} + \frac{\partial u_j}{\partial u_i}\right) \tag{8}$$

Constants used in this model are as follow [23]:

$$\prod_k = C_k f_k \rho \omega K \qquad \prod_\omega = C_2 \rho \omega^2 \qquad S_k = G_k \qquad P_\omega = C_1 f_1 \frac{\omega}{K} P_K \qquad S_\omega = C_3 \frac{\omega}{K} G_K \tag{9}$$

$$\left.\begin{array}{l} C_\mu = 1.0 \qquad C_K = 0.09 \qquad C_1 = 1.92 \qquad C_2 = 0.075 \qquad C_3 = 0.0 \\ \sigma_\omega = 1.3 \qquad \sigma_t = 0.9 \qquad \sigma_k = 2.0 \end{array}\right\} \tag{10}$$

In this model, three damping functions f_μ, f_k, f_1 are added to *k-ω* equations. These functions become small in low Reynolds areas and tend to 1 in high Reynolds areas.

$$f_\mu = \frac{0.025 + \frac{R_t}{6}}{1 + \frac{R_t}{6}} \qquad f_1 = \frac{0.1 + \frac{R_t}{2.7}}{1 + \frac{R_t}{2.7}} f_\mu^{-1} \qquad f_k = \frac{0.278 + (\frac{R_t}{8})^4}{1 + (\frac{R_t}{8})^4} \qquad R_t = \frac{K}{\omega \nu} \tag{11}$$

2.1.3 Boundary Conditions

Generally, boundary conditions to solve the equations are as follow:
On the enclosure's walls:

$$u = v = k = 0$$

$$\omega = \frac{6\nu}{C_2 y^2} \qquad y \to 0$$

Temperature boundary conditions consider constant on hot and cold surfaces:

$\mathrm{T=T_h}$

$\mathrm{T=T_c}$

For adiabatic walls:

$$\frac{\partial T}{\partial y}\Big|_{y=0} = 0$$

$$\frac{\partial \mathrm{T}}{\partial x}\Big|_{x=0} = 0$$

2.2 Solution Procedure

The equations that have already been derived can be used to calculate temperature field and velocity parameters. To conduct calculations in this study, the finite volume is used to discretize the partial differential equations with structural grid [24,25]. A QUICK scheme is employed for the convection terms in the momentum equations and in the thermal energy equation. The convection term in the turbulence transport equations is discretized using the hybrid upwind-central scheme. To increase the accuracy of discretization, a second order Van Leer accuracy method is used [26]. In addition, it

demonstrates that without using damping function G_k and using the combined method, the results will lead to solving the laminar flow in the enclosure. A SIMPLE algorithm is used for the mixed solution of velocity-pressure field, the iterative line-by-line TDMA procedure and the Strongly Implicit Procedure (SIP) are used for the pressure correction equation [27]. To ensure achievement of a steady state, an appropriate under-relaxation technique is used. Due to the use of a low Reynolds number model to solve the velocity field, it requires a sufficient number of grid points to be in the near-wall boundary layer. Special attention has thus been paid to the grid refinement, particularly for computing the buoyancy-driven enclosure flow. In fact, to achieve convergence in the solution equations in this problem, the first approximate grids to the wall should be placed in the near-wall region to resolve the wall-damping effect, this is not necessary for grids farther from the wall [28].

2.3 Grid Study

Running the prepared computer code and considering the high accuracy of solutions, especially near the walls and fluid phase boundaries that cause serious change in some parameters, it is necessary to review the effect of varying the number of grid points on the flow parameters. To achieve this purpose, an enclosure with geometrical specs H=W, H_1=H_5=0.125H, H_2=0.2H, H_3=0.25H, and H_4=0.3H (Fig.1) was used and the Rayleigh number was considered 10^{11} and Pr=0.71. The average Nusselt number of the hot source was determined according to different numbers of the grid points (Table 1). As can be seen in Table 1, the difference between the values obtained using the 100*100 grid and the 110*110 grid are very small and negligible. Thus, a non-uniform grid of 110*110 is selected to run the program.

Table 1: Average Nusselt number of hot source according to the numbers of grid points ($Ra=10^{11}$)

Number of nodes	Average Nusselt of the hot source surfaces
50*50	149.8120
60*60	161.1375
70*70	178.0820
80*80	184.7461
90*90	188.6720
100*100	194.5231
110*110	194.5301

2.4 Validation

To investigate the performance of the computer code in a 2D turbulent state, a comparison was made with two previous studies [5, 16]. In this study, a square enclosure was used with horizontal insulated walls and vertical walls with different temperatures. The cold wall was placed to the right and the hot wall was placed to the left. To solve the equation of turbulent convection flow, a low Reynolds turbulent model k-ω was used. Figures 2 and 3 illustrate the comparison between the results of this study and other studies in this regard. As observed, the obtained results are highly consistent with those of other studies. The difference is at most 1.65% for the average Nusselt number and 1.87% for vertical velocity, which are negligible. To insure the performance of the present model, in another validation we compare the present model with other turbulence models carried

out by Ji [19]. As we can see in Fig. 4, the present model is in good agreement with the others in reference. As the results indicated, the present model is potent to simulate flow in the enclosure at the turbulent and transient stages.

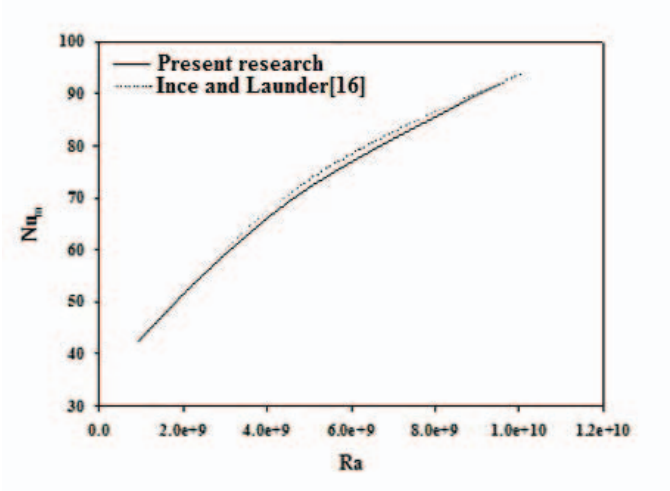

Fig. 2: Variations in the average Nusselt number of heating sources with constant temperature according to changes in Rayleigh number.

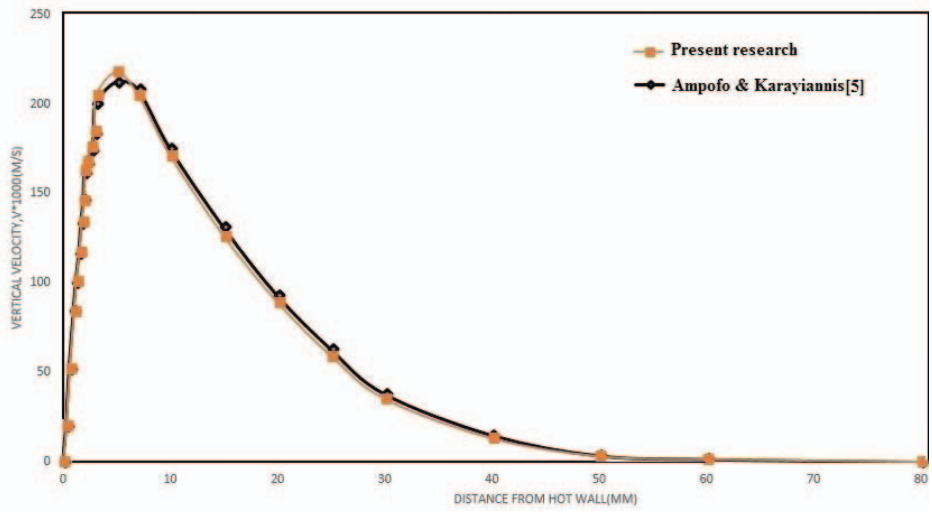

Fig. 3: Variations in vertical velocity according to increase in distance from hot wall.

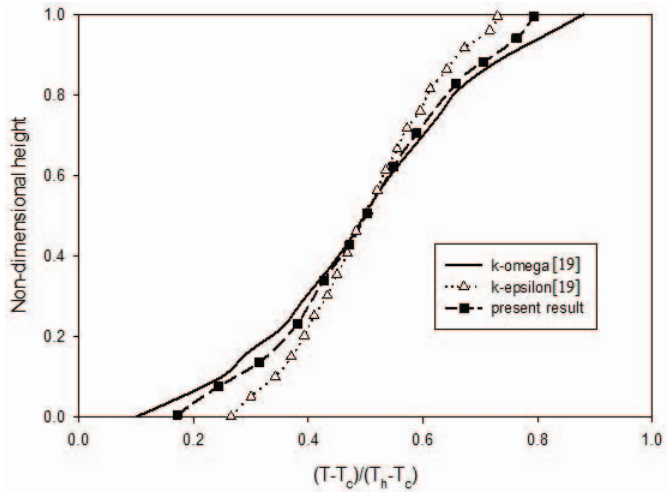

Fig. 4: Numerical comparison between the present model and the reference models [19].

3. RESULTS AND DISCUSSION

3.1 Turbulent Convection Flow in 2D Enclosure

After the performance of the computer code was ensured and appropriate network selected, different runs were conducted at different states. All calculations for air were conducted with Pr= 0.71 and constant geometry enclosure H=W. Rayleigh number varied between 10^9 and 10^{11}. In the following sections, the effects of change in Rayleigh number, heat source position, and heating sources aspect ratio on the rate of heat transfer, isothermal lines, mean velocity in the enclosure, and the maximum values of velocity parameters were investigated.

3.1.1 The Effect of Rayleigh Number

In this section, we changed Rayleigh number only. Geometrical specs H=W, H_1=H_5=0.125H, H_2=0.2H, H_3=0.25H, and H_4=0.3H were considered constant. We investigated the effects of changes in these conditions in any state and illustrated them. Figure 5 indicates isothermal lines and streamlines in this state for different Rayleigh numbers. As illustrated, in 2D turbulent flow inside the enclosure, there was a cold area at the bottom of the enclosure and a hot area at the top. With increasing Rayleigh number from 10^9 to 10^{11}, this condition intensified such that at Rayleigh number 10^{11}, we observed a cooling area besides the right vertical wall. In the area between cold and hot sources, we observed a large heating stress. Further examination of temperature profiles demonstrated that as the Rayleigh number increased, the flows of high and low temperatures between the heating sources mixed better, which caused a more uniform temperature profile at higher Rayleigh numbers compared to lower ones.

Regarding the streamlines, as Fig. 5 illustrates, in all states, there are numerous vortices in the enclosure. Most large vortices form in the area close to hot and cold sources in the middle of the enclosure. Besides the large vortices, we observed several small vortices in the corners of the enclosure that form due to the flow separation in the area near to the wall. Next, we examined the effect of change in Rayleigh number on the heat transfer rate in terms of mean and local Nusselt numbers on the heating sources. Figures 6-8 illustrate the heat transfer rate on hot and cold sources in terms of local and mean Nusselt numbers. As observed, with increasing Rayleigh number, local and mean Nusselt numbers increased in the enclosure. This can be explained by increased velocity parameters due to strengthened buoyancy forces. It is noteworthy (Fig. 8) that because the cold source was bigger than the hot source, its mean Nusselt number that represented the heat transfer rate was lower. To make a more accurate comparison, the results are tabulated in Table 2. In addition to the mean Nusselt numbers of hot and cold sources, the maximum parameters of velocity and mean fluid velocity shown in Table 2.

Table 2: Comparison of temperature and flow parameters for different Rayleigh numbers in turbulent flow.

Ra	**$Nu_{m,h}$**	**$Nu_{m,c}$**	**V_{mean}**	**u_{max}**	**v_{max}**
10^9	50.907	-49.38	0.0148	0.106	0.225
$5*10^9$	98.615	-74.306	0.0273	0.101	0.227
10^{10}	110.33	-84.96	0.0281	0.0901	0.230
$5*10^{10}$	138.10	-107.95	0.0284	0.0894	0.231
10^{11}	195.53	-120.65	0.0287	0.0883	0.234

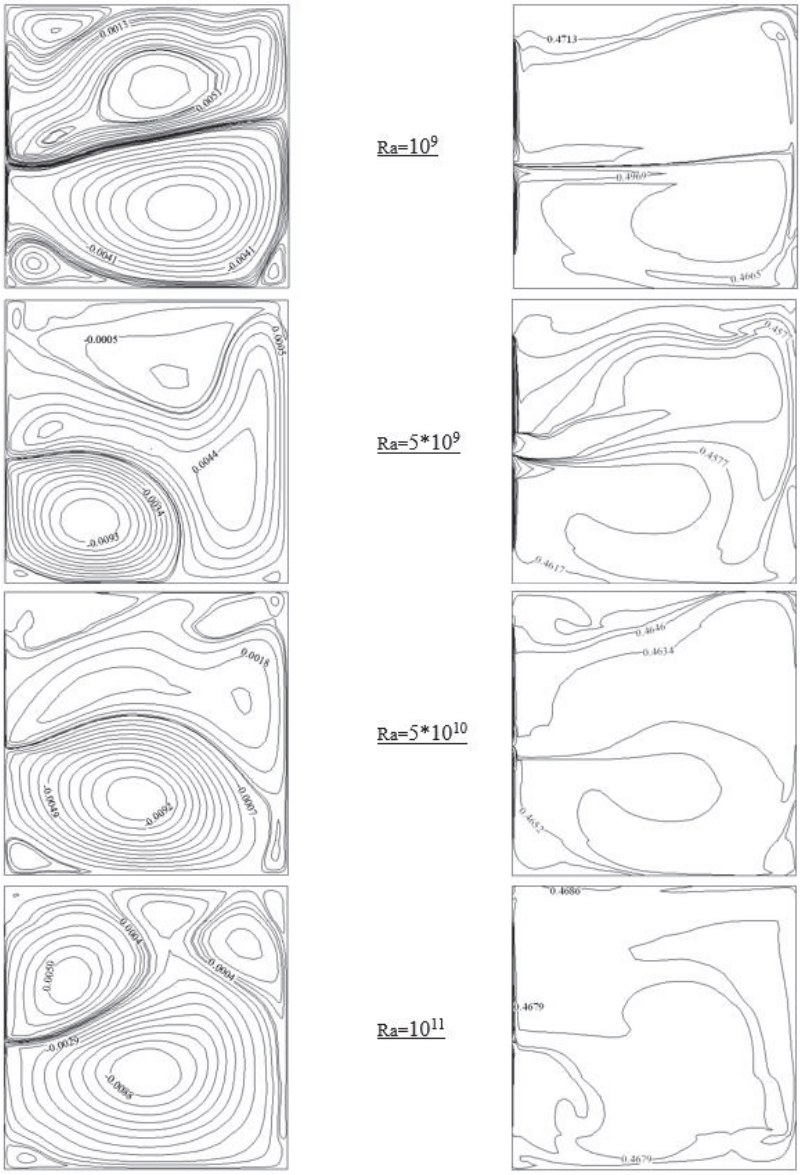

Fig. 5: Isothermal lines (right) and streamlines (left) at different Rayleigh numbers.

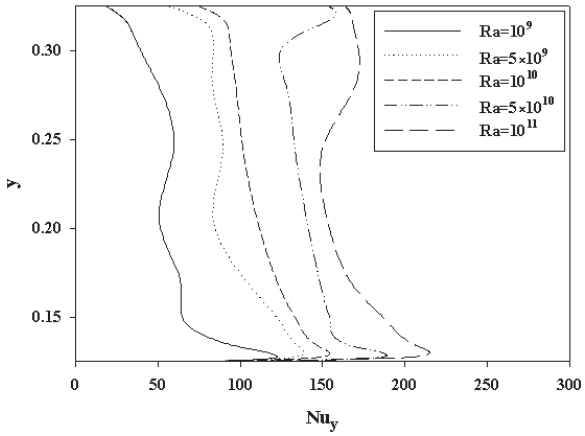

Fig. 6: The effect of changes in local Nusselt number on hot source for different Rayleigh numbers.

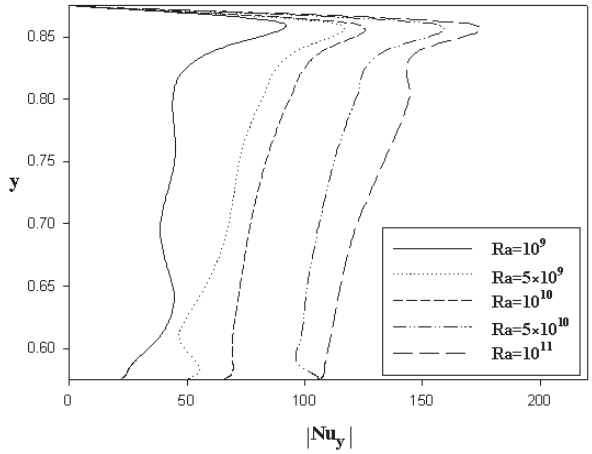

Fig. 7: The effect of changes in the absolute local Nusselt numbers on cold source for different Rayleigh numbers.

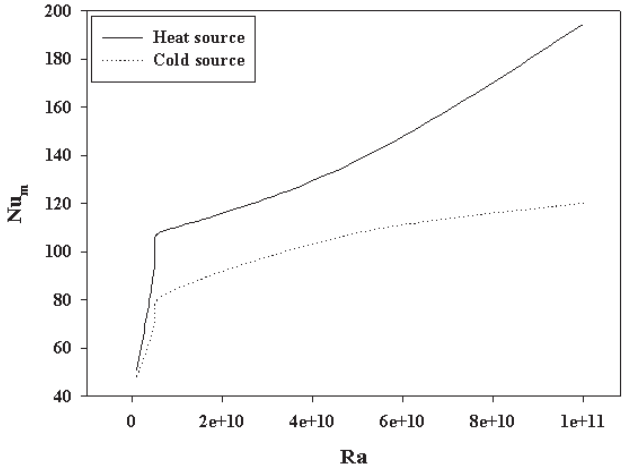

Fig. 8: The mean Nusselt number of heating sources according to changes in Rayleigh number.

As shown in Table 2, with increasing Rayleigh number, maximum horizontal velocity in the enclosure (u_{max}) increased. Due to increased Rayleigh number, this finding is attributed to the acceleration of the fluid velocity in the area between the heating sources due to mixture of cold and hot fluid flows following increased Rayleigh number that in turn causes increase in mean temperature in the enclosure.

3.1.2 Positions of Cold and Hot Sources

Take into consideration the enclosure illustrated in Fig. 1. In this section, we changed the value of H_4, the distance between the two sources. Other geometrical specs H_1=H_5, H_2=0.2H, H_3=0.3H, and H_4=0.3H were assumed constant. In addition, Rayleigh number was considered 10^{11}. In addition to repositioning cold and hot sources on a wall, we also placed the two sources on two opposite walls and then compared heat transfer rates in terms of Nusselt number. Fig.9 illustrates isothermal and stream lines in these states. As stream lines in this figure demonstrate, it was observed that the fluid movement was specified by cell flow in which the upward hot flow jet next to the hot source entered the downward cold source jet next to the cold source. The two flows mixed with each other in the distance between them and the hot flow transferred its heat to the cold flow.Tracing the stream lines when both sources were placed on a single wall, multiple vortices filled

the entire enclosure. With decreasing distance between the heating sources, the number of vortices on the top of the enclosure increased. However, when the two heating sources were placed on two opposite walls, several big standing vortices were observed.

As isothermal lines in Fig. 9 illustrate, when the distance between the two sources decreases, hot air above hot source mixes well with cold air and so, the cold source and the cold air fails to penetrate the enclosure. As a result, a more uniform temperature dissemination occurred in the enclosure. When the two sources were placed on two opposite walls, hot air above the hot source does not mix well with cold air beside the cold source and the cold air could penetrate the enclosure such that low temperature fluid on the bottom of the enclosure assembled with the high temperature fluid on the top of the enclosure. Therefore, the air temperature became less uniform compared to when the two heating sources were placed on a single wall. As illustrated in Fig.10, the rate of heat transfer from cold source to hot source was estimated in terms of mean Nusselt number. As Fig.10 shows, with increasing distance between the sources, the rate of heat transfer from heating sources into the enclosure declined, but these changes were negligible possibly due to decreased velocity parameters in the enclosure.

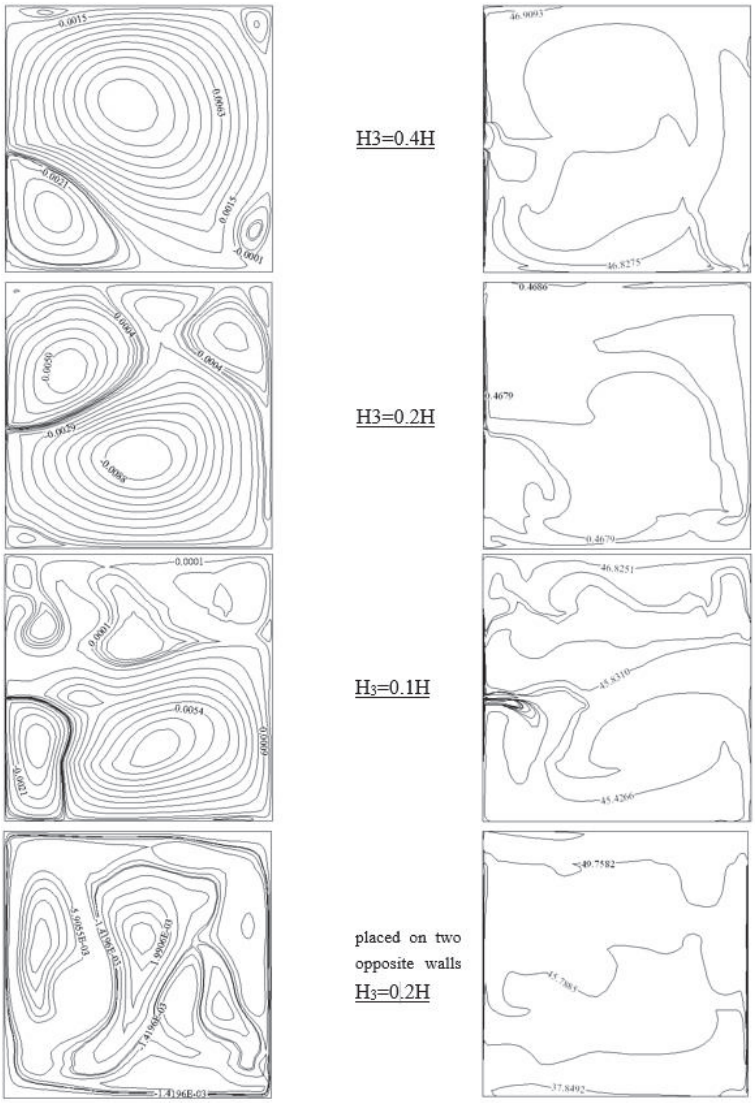

Fig. 9: Isothermal (right) and stream (left) lines in different positions of hot and cold sources ($Ra=10^{11}$).

According to Fig. 11, with increasing distance between the sources, maximum horizontal velocity (u_{max}) and maximum vertical velocity (v_{max}) in the enclosure decreased. This observation can be attributed to the movements of the fluid on the heating sources and the interaction of high temperature fluid with low temperature fluid in the distance between the heating sources. To make a more accurate comparison, the above results were tabulated in Table 3. In addition, Table 3 compares the heat transfer rate between hot and cold sources on two opposite walls. As it can be observed, when the heating sources were placed on two opposite walls, mean Nusselt number increased dramatically, which can be attributed to the regular vortex movement of the fluid in which fluid neighboring the hot source went upward and fluid neighboring the cold source went downward in the enclosure. Because the two heating sources were placed on two opposite walls, the two fluid flows reinforced each other, which led to increased mean velocity of fluid movement in the enclosure. With an increase in mean velocity in the enclosure, the heat transfer rate increased because of the fluid movement.

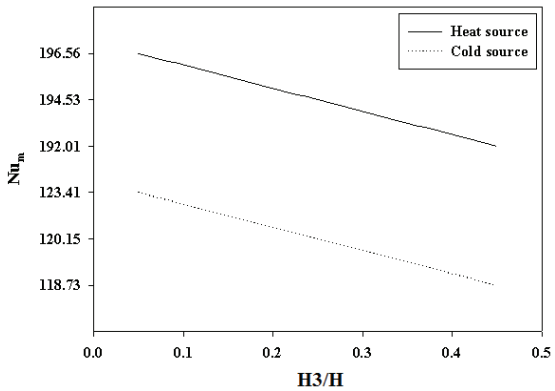

Fig. 10: Changes in mean Nusselt number of hot and cold sources according to changes in distance between heating sources ($Ra=10^{11}$).

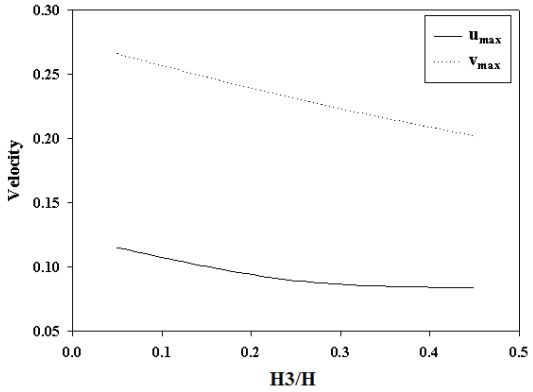

Fig. 11: Changes in maximum parameters of velocity in enclosure according to changes in distance between heating sources ($Ra=10^{11}$).

Table 3: Comparison of heat and flow parameters for different Rayleigh numbers in turbulent flow.

Positions of thermal sources		$Nu_{m,h}$	$Nu_{m,c}$	V_{mean}	u_{max}	v_{max}
Placed on single wall	**H_3=0.4H**	193.08	-121.46	0.0271	0.0855	0.269
Placed on single wall	**H_3=0.2H**	195.61	-124.78	0.0286	0.0915	0.245
Placed on single wall	**H_3=0.1H**	196.98	-128.12	0.0963	0.125	0.209
Placed on two opposite walls H_3=0.2H		212.04	-161.77	0.2108	0.1716	0.281

3.1.3 The Effect of Hot and Cold Sources Aspect Ratio

Assume an enclosure illustrated in Fig. 1. In this section, the length of source is considered constant, H_2=0.2H. By changing the length of the cold source, H_4, we studied the effect of changes in the heating sources aspect ratio. Other geometrical specs, H_3=0.3H and H_1=H_5, were assumed constant and the Rayleigh number was considered to be 10^{11}.

As stream lines in the graphs on the left side of Fig. 12 illustrate, the fluid movement was determined by vortex flow in which the fluid moves upward in parallel with the hot surface and moves downward in parallel with the cold surface. With the change in cold

and hot sources aspect ratio, no marked changes occurred in the stream lines. In all states, two large vortices were formed approximate to the heating sources and the central areas of the enclosure and multiple small vortices formed in the corners of the enclosure. As isothermal lines in the graphs on the right side of Fig.12 illustrate, with an increase in the heating sources aspect ratio, no marked changes occurred in the isothermal lines. Cold fluid that moved alongside gravity acceleration faced hot fluid that moved in the opposite direction of the gravity acceleration in the distance between the two sources such that in all states, a cold area is seen at the bottom, next to the cold source, a hot area is seen at the top, next to the hot source, and an area with uniform temperature profile in the wide central area of the enclosure.

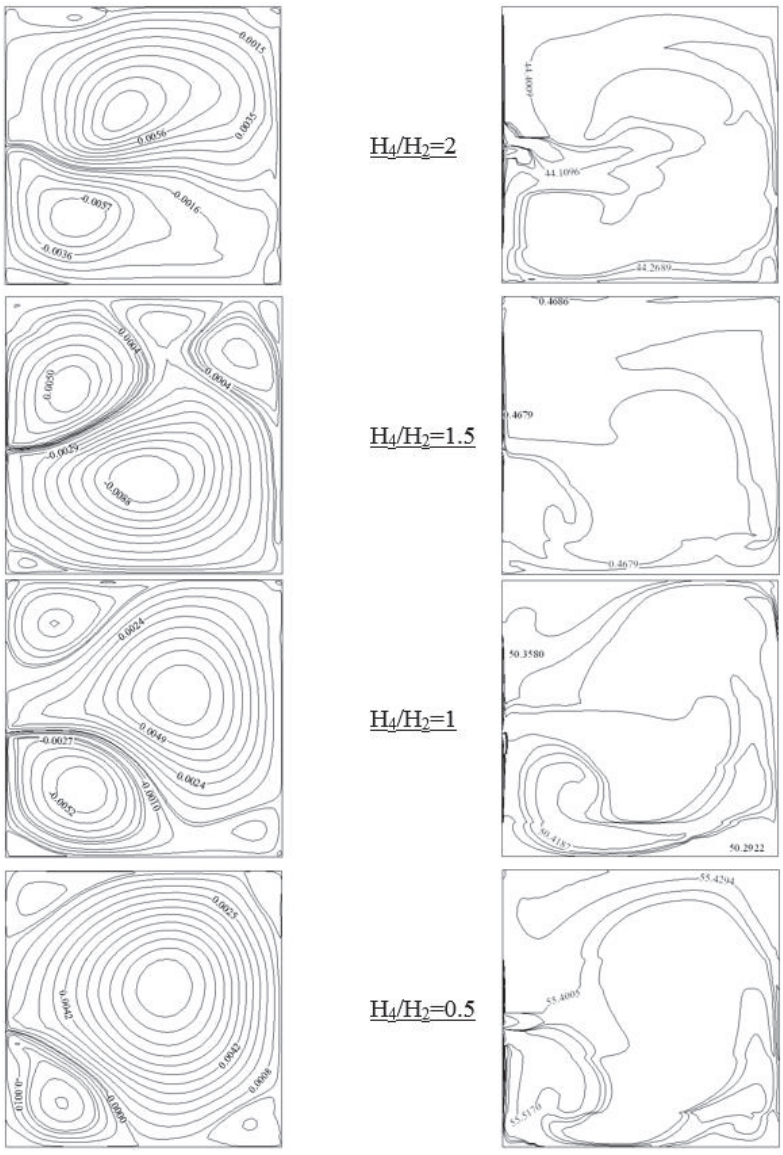

Fig. 12: Isothermal (right) and stream (left) lines in different aspect ratios of cold source to hot source ($Ra=10^{11}$).

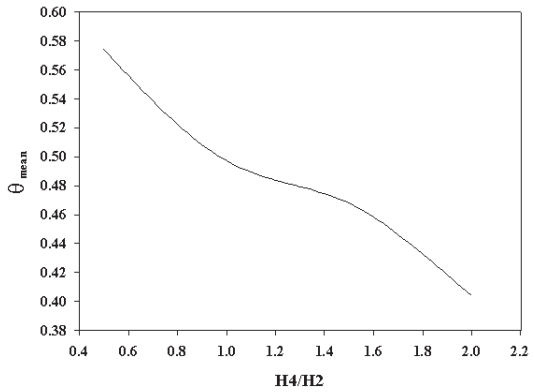

Fig. 13: Changes in mean temperature according to heating sources aspect ratio ($Ra=10^{11}$).

The studies of changes in heating sources aspect ratio on the heat transfer rate indicated that with an increase in the ratio of the length of the cold source to that of the hot source, the heat transfer rate underwent an increasing trend, which can be attributed to the increased parameters of flow in the enclosure. It was also demonstrated that with decreasing aspect ratio, the maximum velocity parameters u_{max} and v_{max} in the enclosure decreased, which in turn caused a decrease in mean temperature in the enclosure. As illustrated in Fig. 13, with increasing aspect ratio, mean dimensionless temperature in the enclosure decreased, which can be explained by the increased area of the cold source that causes a decrease in temperature in the enclosure.

Table 4: The comparison of heat transfer rate and flow parameters in different heating sources aspect ratio in turbulent flow.

sources aspect ratio	$Nu_{m,h} \times Ah$	$Nu_{m,c} \times Ac$	V_{mean}	u_{max}	v_{max}
H_4/H_2=2	42.21	-42.44	0.0314	0.205	0.298
H_4/H_2=1.5	38.74	-38.33	0.0296	0.165	0.278
H_4/H_2=1	35.56	-36.15	0.0214	0.0105	0.248
H_4/H_2=0.5	27.14	-28.11	0.019	0.0951	0.199

4. CONCLUSION

Based on the calculations carried out in this research, the numerical results allow a better understanding on the influence of heating source arrangement within a turbulent natural convection flow in an enclosure. The influence on fluid flow and heat transfer was identified for the different arrangement of the heating sources within the enclosure. Some general conclusions are presented below.

In constant positions of hot and cold sources on a wall, if the Rayleigh number increased, the mean Nusselt number of both heating sources, maximum flow function, and maximum velocity parameters increased.

Study of different positions of hot and cold sources with constant aspects and temperature difference indicated that the dimensionless heat transfer rate increased with a decrease in the distance between the hot and cold sources on a single wall. If the two sources were placed on two opposite walls, a dramatic increase occurred in mean Nusselt number and mean temperature in the enclosure. However, because the distribution of the temperature profile is not uniform, the optimal position of the hot and cold sources is on a single wall with short distance.

Study of different heating sources aspects ratio with constant temperature difference and distance indicated that with an increase in sources aspect, the dimensionless heat transfer rate increased and mean temperature in the enclosure decreased.

REFERENCES

[1] Kadem S, Lachemet A,Younsi R, Kocaefe D. (2011). 3D-Transient modeling of heat and mass transfer during heat treatment of wood. International Communications in Heat and Mass Transfer, 38(6): 717-722.

[2] Laguerre O, Benamara S, Remy D, Flick D. (2009). Experimental and numerical study of heat and moisture transfers by natural convection in a cavity filled with solid obstacles. International Journal of Heat and Mass Transfer, 52(25-26): 5691-5700.

[3] Calcagni B, Marsili F, Paroncini M. (2005). Natural convective heat transfer in square enclosures heated from below. Applied Thermal Engineering, 25(16): 2522-2531.

[4] Tian YS, Karayiannis TG. (2000). Low turbulence natural convection in an air filled square cavity - Part II: The Turbulence Quantities. International Journal of Heat and Mass Transfer, 43(6): 867-884.

[5] Ampofo F, Karayiannis TG. (2003). Experimental benchmark data for turbulent natural convection in an air filled square cavity. International Journal of Heat and Mass Transfer, 46(19): 3551-3572.

[6] Dafa Alla AA, Betts PL. (1996). Experimental study of turbulent natural convection in a tall air cavity. Experimental Heat Transfer, 9(2): 165-194.

[7] Penot F, Skurtys O, Saury D. (2010). Preliminary experiments on the control of natural convection in differentially-heated cavities. International Journal of Thermal Sciences, 49(10): 1911-1919.

[8] Chen W, Liu W. (2004). Numerical and experimental analysis of convection heat transfer in passive solar heating room with greenhouse and heat storage. Solar Energy, 76(5):623-633.

[9] Saury D, Rouger N, Djanna F, Penot F. (2011). Natural Convection in an Air-Filled Cavity: Experimental Results at Large Rayleigh Numbers. International Communications in Heat and Mass Transfer, 38(6): 679-687.

[10] Barakos E, Mitsoulis G, Assimacopoulos D. (1994). Natural-Convection Flow in a Square Cavity Revisited- Laminar and Turbulent Models with Wall Functions. International Journal for Numerical Methods in Fluids, 18(7): 695-719.

[11] Elder JW. (1965). Turbulent free convection in a vertical slot. J. Fluid Mechanics, 23(1): 99-111.

[12] Giel PW, Schmidt W. (1986). Experiment study of high Rayleigh number natural convection in an enclosure. 8th International heat transfer conference, 4: 1459-1464.

[13] Cheesewright R. (1968). Turbulent natural convection from a vertical plane surface. J. Heat Transfer, 90(1): 1-6.

[14] Olsen DA, Glicksman LR, Ferm HM. (1990). Steady state natural convection in an empty and partitioned enclosure at high Rayleigh numbers. J. Heat Transfer, 112(3): 640-647.

[15] Chen Q. (1996). Prediction of room air motion by Reynolds-Stress models. Building and Environment, 31: 233-244.

[16] Ince NZ, Launder BE. (1989). On the computation of buoyancy-driven turbulent flows in rectangular enclosures. International journal of heat and fluid flow, 10(2): 110-117.

[17] Hanjealic K, Vasc E. (1993). Computation of Turbulent natural convection in rectangular Enclosure with algebraic flux model. Interntional Journal of Heat and Mass Transfer, 36(14): 3603-3624.

[18] Sigey JK, Gatheri FK, Kinyanjui M. (2004). Numerical study of free convection turbulent heat transfer in an enclosure. Energy Conversion and Management, 45(15-16): 2571-2582.

[19] Ji Y. (2014). CFD Modelling of Natural Convection in Air Cavities. CFD Letters, 6(1): 15-31.

[20] Henkes RAWM, Van Der Vlugt FF, Hoogendoom FF. (1991). Natural convection flow in a square cavity calculated with low-Reynolds-number turbulence models. International Journal of Heat and Mass Transfer, 34(2): 377-388.
[21] Penot F, Skurtys O, Saury D. (2010). Preliminary experiments on the control of natural convection in differentially-heated cavities. International Journal of Thermal Sciences, 49(10): 1911-1919.
[22] Versteeg HK, Malalasekera W. (2007). An Introduction to Computational Fluid Dynamics. The Finite Volume Method Approach, Pearson education limited, USA, 2th Ed.
[23] [23] Wilcox DC. (1994). Simulation of transition with a two-equation turbulence model. AIAA Journal, 32(2): 247-255.
[24] Davidson L, Farhanieh B. (1991). CALC-BFC: A finite-volume code employing collocated variable arrangement and Cartesian velocity components for computation of fluid flow and heat transfer in complex three-dimensional geometries. Report 92/4, Department of Thermo and Fluid Dynamics, Chalmers University of Technology, Gothenburg, Sweden.
[25] Ahmadi M. (2017). Natural Convective Heat Transfer in a Porous Medium within a Two Dimension Enclosure. IIUM Engineer Journal, 18(2): 196–211.
[26] Van Leer B. (1974). Towards the ultimate conservative difference scheme: Monotonicity and conservation combined in a second order scheme. Journal of Computational Physics, 14(4): 361-370.
[27] Ahmadi M, Khosravi Farsani A. (2018). CFD Simulation of Non-Newtonian Two-Phase Fluid Flow Through a Channel with a Cavity. Thermal science, online First. DOI:10.2298/TSCI180102151A
[28] Hoffmann KA, Chiang ST. (1993). Computational fluid dynamics for engineers. Engineering Education System, Wichita, USA.

NOMENCLATURE

W	Width of the enclosure in x-direction	m
H	Height of the enclosure in y-direction	m
T	Temperature	°C
T_h	Hot Temperature	°C
T_c	Cold Temperature	°C
P	Pressure	Pa
X, Y	Cartésien coordinats	-
U, V	Cartesian velocities	$m.s^{-1}$
Cp	Specific heat capacity at constant pressure	J/Kg.k
K	Turbulent kinetic energy	-
g	Acceleration of gravity	m/s^2

i) Greek Symbols

ν	Kinematic viscosity	$m^2.s^{-1}$
ρ	Density	kg/m^3
ω	Specific dissipation rate of K	-
μ	Dynamic viscosity	Pa.s
α	Fluid thermal diffusivity	$m^2.s^{-1}$

ii) Dimensionless Numbers

Ra	Rayleigh number, $(= g \beta (T_h-T_c) H^3 / \nu\alpha)$	-
Nu	Local Nusselt number, $(= h_{conv} H/k)$	-
Nu_m	Average Nusselt number, $(= \int Nu\ dA)$	-
Pr	Prandtl number, $(= \nu/\alpha)$	-